

## Low frequency excitation in amorphous acrylic polymers

F. Viras and T. A. King

Physics Department, Schuster Laboratory, University of Manchester, Manchester, M13 9PL, UK

(Received 12 July 1983; revised 5 October 1983)

Low frequency Raman depolarized spectra from poly(methyl methacrylate) have been determined at temperatures between 293 K and 85 K in the frequency region  $5 \text{ cm}^{-1} < \bar{\nu} < 200 \text{ cm}^{-1}$ . All the reduced intensity spectra resolve into two bands: a broad and intense band at  $91 \text{ cm}^{-1}$  and a narrower and weaker band at  $22 \text{ cm}^{-1}$ . The Raman intensities do not depend on temperature which implies first order Raman scattering. Room temperature low frequency Raman spectra were also recorded from poly(ethyl methacrylate) and poly(-n-butyl methacrylate). In the two PMMA substitutes the high frequency band is shifted to lower values as the side group mass is increased and show a Debye-like character. The lower frequency band cannot be resolved in the spectrum of PEMA and PnBMA. The two bands at  $91 \text{ cm}^{-1}$  and  $22 \text{ cm}^{-1}$  are attributed to side group and backbone motions respectively. By studying PMMA samples of different tacticity no dependence of the band frequency on chain configuration has been detected. The density of states  $g(\omega)$  obtained through the low frequency Raman spectrum has been used to calculate the specific heat  $C_v$ . The values of  $C_v$  obtained are lower than those measured calorimetrically but varied with temperature in a similar manner in the region  $0.8 < T < 4\text{K}$ .

(Keywords: Raman; amorphous; poly(methyl methacrylate); specific heat; density of states; phonon modes)

### INTRODUCTION

Raman scattering spectra observed at low frequencies ( $0\text{--}200 \text{ cm}^{-1}$ ) have revealed a broad feature in some inorganic<sup>1-5</sup> and polymer glasses<sup>6-10</sup> which is absent in the spectra of the solids in the crystalline phase. Recently the same phenomenon has been observed from some organic liquids<sup>11-13</sup>. Otherwise very little work on low frequency Raman scattering from amorphous polymers has been reported. The nature of the scattering mechanisms responsible for those broad bands are not yet well known. It is believed that they are related to heat transferring modes causing the excess in the specific heat which is characteristic of the amorphous phase. The low frequency Raman spectrum can give very useful information about the heat carrying vibrational modes at very low temperatures. A considerable number of models have been proposed to explain the anomalous specific heat in amorphous materials.

The specific heat of amorphous solids at very low temperatures does not follow the theory of Debye for crystals<sup>14</sup> but has values much higher than a  $T^3$  behaviour predicts<sup>15-24</sup>. The constant volume molar specific heat is given in the quasi-harmonic approximation by

$$C_v = k \int_{\omega_{\min}}^{\omega_{\max}} g(\omega) \left( \frac{\hbar\omega}{kT} \right)^2 \frac{e^{-\hbar\omega/kT} d\omega}{[e^{-\hbar\omega/kT} - 1]^2} \quad (1)$$

Here  $g(\omega)$  is the density of states and  $k$  Boltzmann's constant.

The mechanical disorder has been considered by Shuker and Gammon<sup>24</sup> to relate the light scattering

intensities with the density of states  $g(\omega)$  through

$$I_{\alpha\beta\gamma\delta}(\omega, T) = \sum_b C_b^{\alpha\beta\gamma\delta} g_b(\omega) \left[ \frac{\eta(\omega, T) + \binom{1}{0}}{\omega} \right] \quad (2)$$

The 1 and 0 in parenthesis refer to the Stokes and anti-Stokes spectrum respectively,  $\eta(\omega, T)$  is the Bose-Einstein factor given by

$$\eta(\omega, T) = [\exp(\hbar\omega/kT) - 1]^{-1} \quad (3)$$

The coupling coefficient  $C_b$  depends on the polarization geometry of the incident and scattered light, in the low frequency part of the spectrum it varies as<sup>25,26</sup>

$$C_b \sim \omega^2 \quad (4)$$

Here  $b$  identifies groups of similar normal vibrations. The  $\omega^2$  dependence of the coupling coefficient has been previously suggested by the model calculations of Whalley and Bertie<sup>27</sup>.

The reduced Stokes spectrum is calculated through

$$I_R = I_{\text{obs}} \omega [1 - e^{-\hbar\omega/kT}] \quad (5)$$

According to equations (2) to (5) the function  $I_R/\omega^2$  will be proportional to the density of states.

$$I_R/\omega^2 \sim \sum_b g_b(\omega) \quad (6)$$

Thus determination of  $I_R$  leads to information on  $g(\omega)$ .

**Table 1** Sample characterization. Ratios of the triad sequences are given

Sample	Molecular weight	Tacticity mm : rr : mr	Crystallinity	Source
PMMA - 1	12 000	93 : 3 : 4	53%	CNRS
PMMA - 2	13 000	51 : 28 : 21	amorphous	CNRS
PMMA - 3	95 000	4 : 55 : 41	amorphous	CNRS
PMMA - 4	10 <sup>6</sup>	5 : 60 : 35	—	ICI
PEMA	270 000	5 : 65 : 30	—	Polysciences
PnBMA	200 000	5 : 65 : 30	—	Polysciences

## EXPERIMENTAL

Low frequency depolarized Raman spectra ( $0 < \bar{\nu} < 200 \text{ cm}^{-1}$ ) were obtained from a Cary 82 triple monochromator spectrometer working with an argon-ion laser (model 164 Spectra-Physics). The excitation line was the 514.5 nm wavelength with an output power between 400 and 600 mW. The low temperature Raman scattering measurements were made using a continuous flow cryostat (Oxford Instruments CF 104) giving a temperature precision of  $\pm 2 \text{ K}$  over the period of recording of the spectrum. Due to the temperature gradient between the position of the temperature sensor and the scattering volume within the sample, there was an estimated uncertainty in the temperature of  $\pm 5 \text{ K}$ .

Four samples of PMMA were studied having various molecular weight, tacticity and degree of crystallinity, together with two substitutes, PEMA and PnBMA (Table 1). The data contained in Table 1 was obtained by the sample characterization methods of gel permeation chromatography for the determination of molecular weight, nuclear magnetic resonance for characterising the tacticity and wide-angle X-ray scattering for the determination of sample crystallinity. It is expected that stereoregularity along the chain is a prerequisite to the formation of a well developed crystal structure. The PMMA samples from 1 to 3 and poly(ethyl methacrylate) were powders, poly(n-butyl methacrylate) consisted of small beads and PMMA sample 4 was a clear solid of high optical quality cut in a cubic shape of dimensions  $1 \text{ cm} \times 1 \text{ cm} \times 1 \text{ cm}$  and polished to a good optical finish.

## RESULTS

### Reduced Raman scattering intensities and density of states for PMMA

Raman depolarized spectra from solid amorphous PMMA sample 4 recorded at temperatures of 293 K, 200 K, 107 K and 85 K in the low frequency region from about  $5 \text{ cm}^{-1}$  to  $200 \text{ cm}^{-1}$  are shown in Figure 1. All the spectra have broad peaks characteristic of an amorphous structure. At 293 K two peaks are well distinguishable in the observed spectrum: one at  $\sim 70 \text{ cm}^{-1}$  and the other at  $\sim 17 \text{ cm}^{-1}$ . The picture is quite different in the reduced intensity spectrum as seen in Figure 2. There is no significant temperature dependence of the reduced intensities within experimental error. This is evidence that Raman scattering from amorphous PMMA in the low frequency region is a first order process<sup>28</sup>.

Due to the lack of information about the Raman spectrum at frequencies  $\bar{\nu} \sim 0$ , an approximation has to be made for the Rayleigh wing, which is thus extrapolated to the base line as in Figure 3. A similar procedure has been followed by Fraser<sup>29</sup> and Snyder *et al.*<sup>30</sup> for the shape of

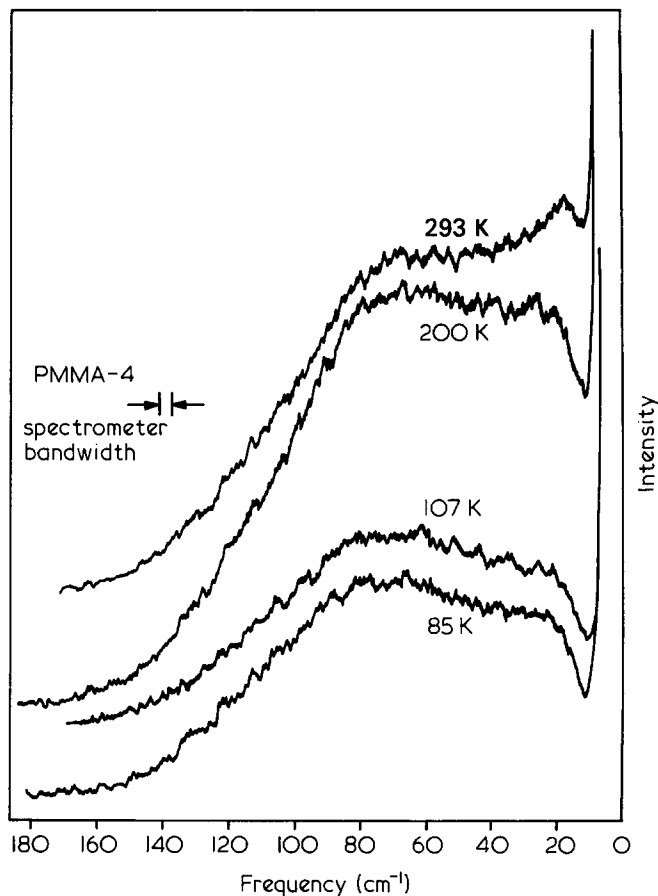


**Figure 1** Low frequency Raman scattering from amorphous PMMA (sample 4) as a function of temperature. Spectral resolution =  $3 \text{ cm}^{-1}$

the Rayleigh wing near zero shift. The reduced intensity spectrum is then resolved into two peaks by following the procedure adopted by Furukawa *et al.*<sup>4</sup> (in the study of the high frequency Raman spectrum of silicate glasses). In Figure 3 the two overlapping peaks are resolved by correcting the stronger one at  $91 \text{ cm}^{-1}$  to a symmetrically shaped peak. The two peaks have been shifted to  $\sim 91 \text{ cm}^{-1}$  and  $22 \text{ cm}^{-1}$  respectively; the shift has been introduced by the two correction factors for temperature ( $1 - e^{-h\omega/kT}$ ) and for frequency  $\omega$ .

The band observed at  $70 \text{ cm}^{-1}$  ( $91 \text{ cm}^{-1}$  in the reduced intensity spectrum) was first reported in 1953 by Roy<sup>6</sup> and later by Spells and Shepherd<sup>8</sup> from Raman scattering spectroscopy. Incoherent inelastic neutron scattering, which provides information on the vibrational density of states<sup>31</sup> and enables comparison between optical and neutron spectra<sup>32,33</sup>, has revealed a concentration of vibration density of states at  $\sim 100 \text{ cm}^{-1}$  associated with the ester group. No attempt has been reported in

Low frequency Raman scattering from PMMA substitutes

The low frequency Raman scattering spectra of poly-(ethyl methacrylate) and poly(n-butyl methacrylate) were recorded at 293 K and are shown in Figure 5. The Rayleigh wing of these samples is broad and overlaps the lower frequency part of their spectrum. The 293 K spectrum of PMMA sample 1 has been added in Figure 5 for comparison. The difference in the spectra of these

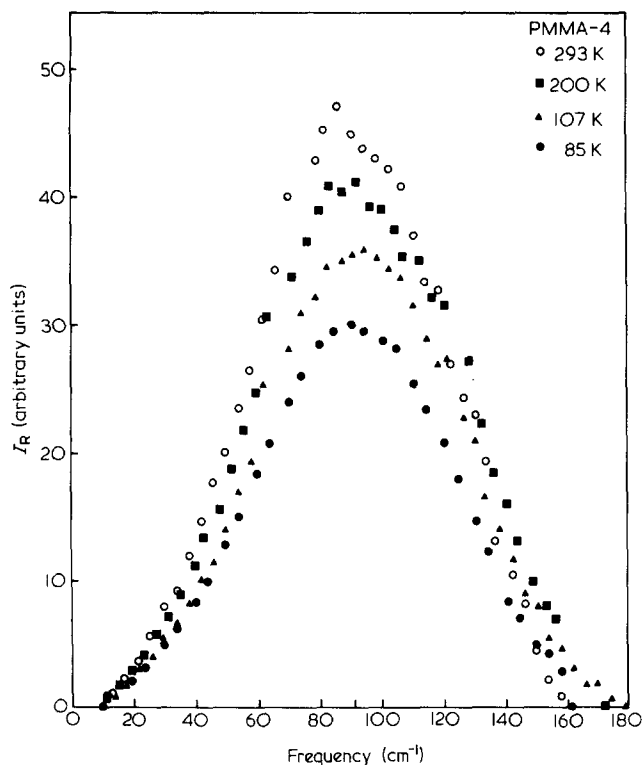


Figure 2 Reduced Raman intensities of amorphous PMMA (sample 4) for temperatures of 85 K to 293 K

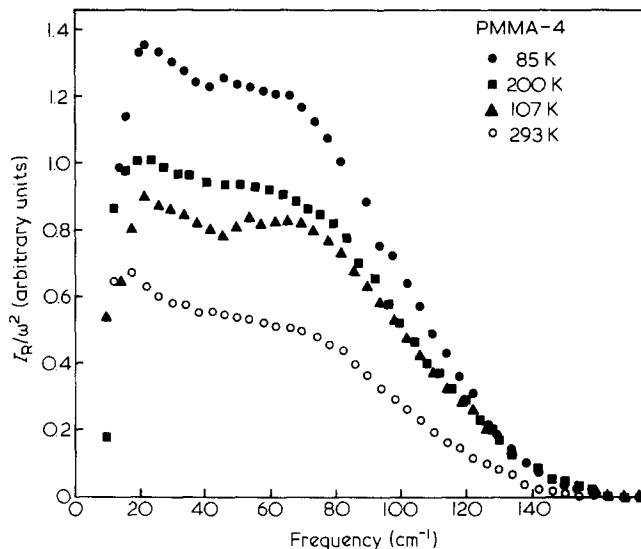


Figure 4 Frequency variation of  $I_R/\omega^2$  for amorphous PMMA sample 4. The ordinate scales are arbitrary for the different temperatures

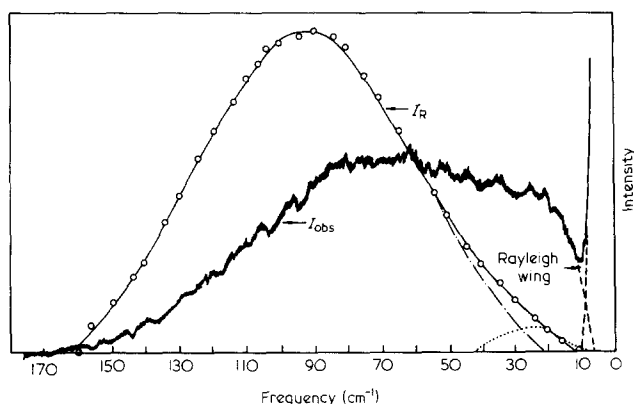


Figure 3 Low frequency Raman spectrum of PMMA-4 and corresponding reduced intensity at 85 K for a Rayleigh wing cut-off frequency of  $6\text{ cm}^{-1}$ . Intensity difference peak (.....)

assigning the weaker peak at  $17\text{ cm}^{-1}$  ( $22\text{ cm}^{-1}$  in the  $I_R$  spectrum) to a particular scattering mechanism.

The density of states related to the scattering of light in the low frequency region, premultiplied by a scaling factor  $c_b$ , is obtained from the Raman scattering spectrum through the function  $I_R/\omega^2$ . It is usually considered that  $c_b$  is constant over the whole of the low frequency spectrum. Figure 4 shows the function  $I_R/\omega^2$  (on an arbitrary scale) at four temperatures over the range 293–85 K. The quantity  $I_R/\omega^2$  is calculated for cut-off frequencies from 1 to  $9\text{ cm}^{-1}$  at  $1\text{ cm}^{-1}$  intervals and normalized to unity. No significant temperature dependence of the density of states is detected and this supports the first order Raman scattering mechanism from amorphous PMMA. Two features are distinguishable: a broad shoulder extending from  $30\text{ cm}^{-1}$  up to the higher frequencies of the spectrum and a narrow band appearing at the lower frequency region.

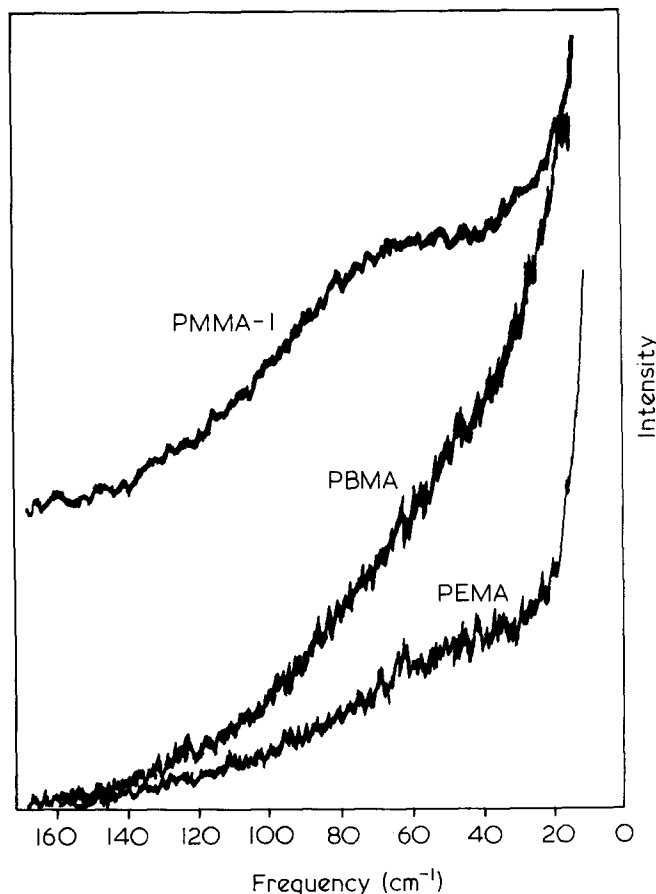


Figure 5 Low frequency Raman spectra from PEMA, PBMA and PMMA-1 at 293 K. Spectral resolution =  $3\text{ cm}^{-1}$

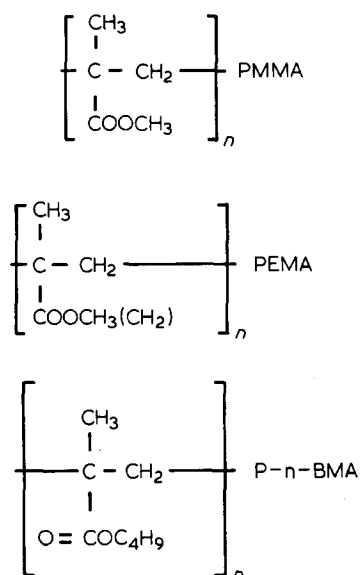


Figure 6 Structure of the repeat unit for PEMA, PBMA and PMMA

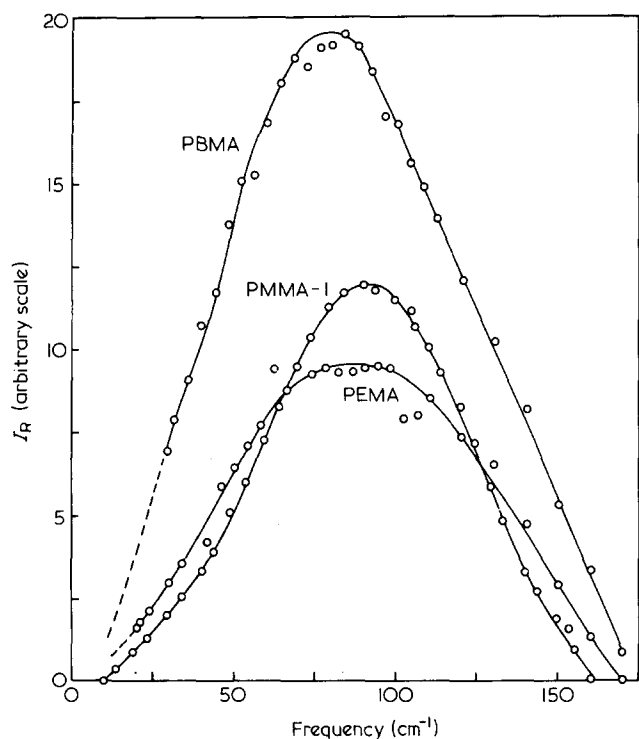


Figure 7 Reduced Raman intensities for PEMA, PBMA and PMMA-1 for the spectra shown in Figure 5

samples is striking; the spectrum of the two substitutes is not as broad as the spectrum of PMMA and the observed relative intensities around  $70 \text{ cm}^{-1}$  become less strong as the side group of the repeat unit of the polymer becomes heavier, as indicated in Figure 6.

In Figure 7 the reduced depolarized intensities from PMMA sample 1, PEMA, PnBMA show a clear shift of the frequency of the maximum towards lower values as the weight of the repeat unit increases. The  $I_R$  curves of PEMA and PnBMA are more symmetric than PMMA about the maximum, and hence they cannot be resolved into two peaks. The Rayleigh wing is of higher intensity for the substitutes PEMA and PnBMA and may obscure the second peak. It is possible that there is another low

frequency and weak peak which has been shifted to even lower frequencies as the side group mass increases and which overlaps with the strong Rayleigh wing and therefore is hidden.

The density of state functions  $I_R/\omega^2$  (for the three samples) show a distinct difference as seen in Figure 8. The band observed at high frequencies in the spectrum of PMMA is absent in the spectra of its substitutes with evidence of a shift to even lower frequencies as the side group weight increases.

The frequencies  $\bar{\nu}_2$ , where the stronger reduced Raman intensity band occurs, shows a  $M_0^{-1/3}$  dependence, where  $M_0$  is the monomer unit weight, as indicated in Figure 9. Values for  $\bar{\nu}_2$  and  $M_0$  are shown in Table 2 and also the frequencies  $\bar{\nu}$  corresponding to the calculated Debye frequencies through the equation<sup>34</sup>:

$$\bar{\nu} = \frac{v}{2\pi c} [2\pi^2 N_0 \rho / M_0]^{1/3} \left( \frac{n}{m} \right)^{1/3} \quad (7)$$

where  $v$  is the mean sound velocity,  $c$  is the speed of light,  $N_0$  Avogadro's number,  $\rho$  is the mean density of the polymer,  $n$  the number of degrees of freedom for each

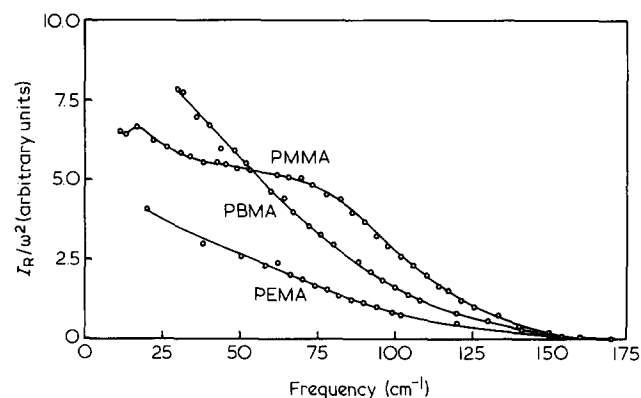


Figure 8 Frequency variation of  $I_R/\omega^2$  for PEMA, PBMA and PMMA (sample 1) at 293 K

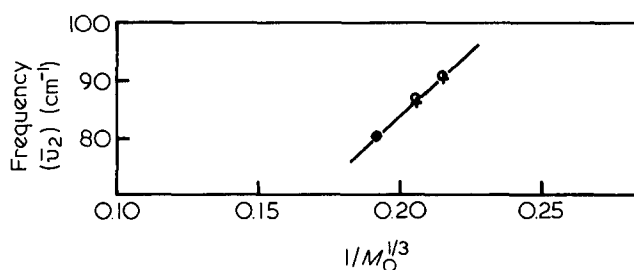
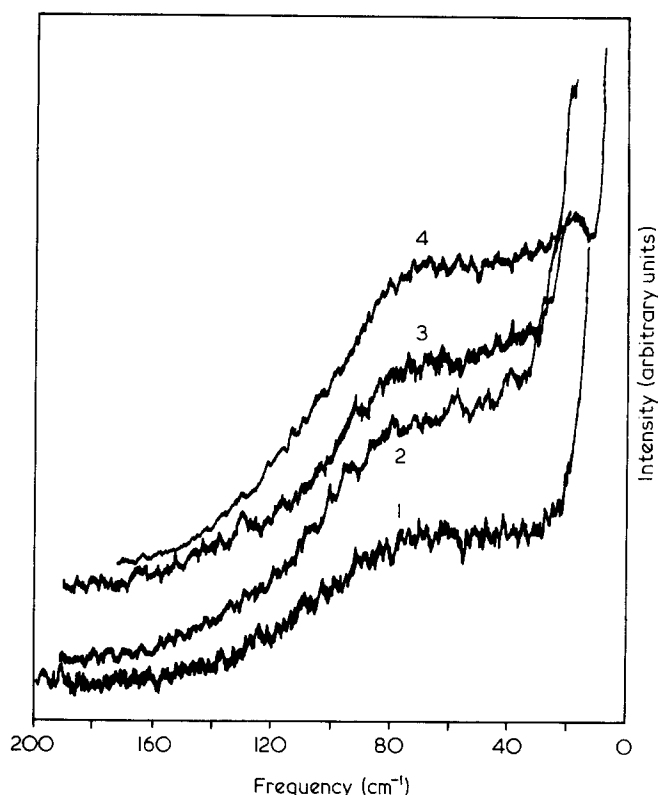


Figure 9 Peak frequency of reduced Raman intensity as a function of  $M_0^{-1/3}$  ( $M_0$  = monomer molecular weight) for PEMA, PBMA and PMMA. Experimental values (O), calculated (+)

Table 2 Frequencies of the reduced Raman intensity peaks  $\bar{\nu}_2$  and calculated Debye frequencies  $\bar{\nu}$  with values of monomer molecular weights

Sample	$\bar{\nu}_2$ (cm <sup>-1</sup> )	$\bar{\nu}$ (cm <sup>-1</sup> )	$M_0$
PMMA - 1 to 4	91.0	90.1	100
PEMA	88.0	86.3	114
PnBMA	80.0	80.2	142



**Figure 10** Raman spectra from PMMA at 293 K. (1) isotactic (sample 1), (2) isotactic/syndiotactic (sample 2), (3) atactic (sample 3) and (4) predominantly syndiotactic (sample 4)

vibration unit and  $m$  the number of molecules in each vibrating unit. The sound velocity and mean density were obtained from Stephens<sup>21</sup> and the same values assumed for PEMA and PnBMA.

For polymers the repeat unit is often taken as the vibration unit<sup>35</sup>, in which case  $m=1$  to a first approximation and  $n=6$ . The Debye frequencies are also shown in Figure 9. It is apparent that Raman scattering measurements from PMMA and its two substitutes are in good agreement with the theory assuming elastic vibrations as heat carriers, in a similar way to lattice vibrations in crystals.

Further Raman data from polycarbonate of bisphenol A, poly(vinylalcohol) and poly(vinylchloride)<sup>36</sup> give important additional information about the behaviour of the very low frequency peak. These three polymers also resolve their low frequency Raman scattering spectrum into two peaks of varying relative peak intensity. The frequencies  $\bar{\nu}_1$  (at which the weak peak occurs) vary inversely as the fraction of the side group mass in the repeat unit. The relative intensities of  $\bar{\nu}_1$  show a similar behaviour, giving evidence that this peak is closely related to the backbone motion of the chain.

#### Influence of tacticity

Raman spectra of four samples of poly(methyl methacrylate) of various tacticities recorded at room temperature are presented in Figure 10. As shown in Table 1, the tacticities of these samples vary from highly isotactic to predominantly syndiotactic and atactic samples. If we exclude the case of PMMA sample 4, for which the good optical quality allows the weak and very low frequency peak to appear in the reduced intensity spectrum, the other PMMA samples have the same spectral features, at

least in the area where the strong Rayleigh band does not distort the scattering intensities. Nevertheless the low frequency narrow band (at  $17\text{ cm}^{-1}$ ) can still be distinguished on the Rayleigh shoulder as a weak modulation on the wing. In the low frequency region ( $\bar{\nu} < 200\text{ cm}^{-1}$ ) the wavelength is too long to 'see' the configurational details inside the monomer unit.

#### Far infra-red absorption in PMMA, PEMA and PnBMA

The difference observed in the Raman spectra from PMMA, PEMA and PnBMA are distinguishable in the far infra-red spectra with slight variations. The bands at  $\sim 100\text{ cm}^{-1}$  and  $\sim 25\text{ cm}^{-1}$  are again observable in the f.i.r. spectrum of PMMA but not in the f.i.r. spectra of PEMA and PnBMA. A continuous increase of the f.i.r. absorbance of PEMA with increasing wave number is observed from about  $5\text{ cm}^{-1}$  to about  $200\text{ cm}^{-1}$ . For PnBMA the f.i.r. spectrum appears to have a very weak and broad band at about  $40\text{ cm}^{-1}$ .

## DISCUSSION

#### Specific heat of PMMA at low temperatures

The low frequency Raman scattering spectrum provides information about  $g(\omega)$  the number of modes in the frequency region between  $\omega$  and  $\omega+d\omega$  and per unit mass. By assuming that the coefficient  $c_b$  has the same value over the frequency range of the spectrum the density of states  $g(\omega)$  may be substituted into equation (1) to obtain  $C_v$ . The upper integration limit is well defined; the lower limit  $\omega_{\min}$  is obscured through overlapping with the Rayleigh line. An approximation is therefore needed for the lower cut-off frequency which is thus used as a fitting parameter<sup>37</sup>. The normalized  $I_R/\omega^2$  is identified with the density of states  $g(\omega)$  of one repeat unit. If it is assumed a vibrating unit is the repeat unit of the polymer and that all repeat units contribute to the spectrum then the density of states is

$$g(\omega) = Ng_N(\omega) \quad (8)$$

where  $N$  is the number of repeat units per unit of polymer. The specific heat in equation (1) then becomes

$$C_v = kN \int_{\omega_{\min}}^{\omega_{\max}} g_N(\omega) \left(\frac{\hbar\omega}{kT}\right)^2 \frac{e^{-\hbar\omega/kT} d\omega}{[e^{-\hbar\omega/kT} - 1]} \quad (9)$$

The calculated  $g_N(\omega)$  is introduced into equation (9), the integration is carried through by an appropriate computer program and values of  $C_v$  obtained as a function of temperature. Figure 11 gives the specific heat plotted as a function of  $C/T^3$  against  $T^2$ :

$$\frac{C(T)}{T^3} = \left(\frac{C}{T^3}\right)_D + \left(\frac{C(T)}{T^3}\right)_R \quad (10)$$

where

$$\left(\frac{C}{T^3}\right)_D = \frac{2\pi^2}{5} \cdot \frac{k^4}{\hbar^3 \rho v_D^3}$$

Here  $\rho$  is the mass density of the polymer,  $v_D$  is the mean sound velocity and  $(C(T)/T^3)_R$  is the calculated specific heat from Raman measurements. Figure 12 shows the

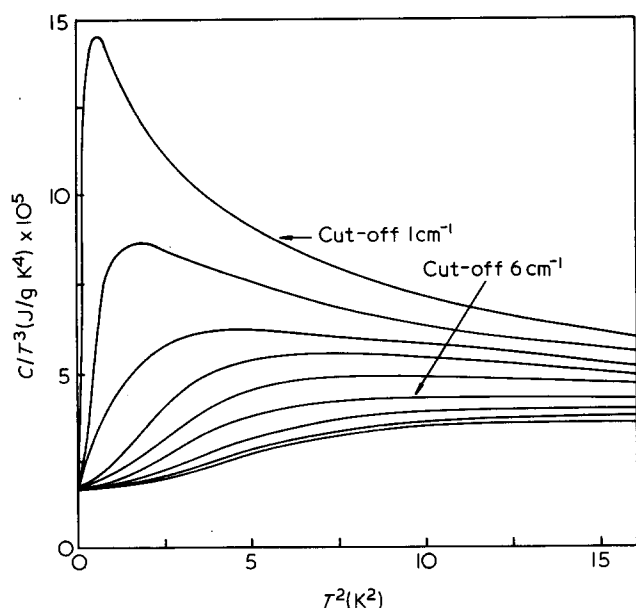


Figure 11 Function  $C_v/T^3$  of amorphous PMMA (sample 4) as a function of  $T^2$  for cut-off frequencies of 1 to 9  $\text{cm}^{-1}$  in  $1 \text{ cm}^{-1}$  intervals

calorimetrically measured specific heat data<sup>18,21</sup>. The curve shows two distinct regions: one between 0.8 and 4 K and the other over temperatures 0.15 to 0.8 K. The higher temperature point of the curve varies weakly with temperature; the second part shows a strong dependence inversely proportional to  $T^2$ . No temperature dependence of the function  $I_R/\omega^2$  in the temperature region  $85 \text{ K} < T < 293 \text{ K}$  has been observed. We may therefore expect no significant changes to occur in the density of states for temperatures as low as 1 K. Information can then be deduced on the specific heat at temperatures as low as 1 K from Raman data at 85 K.

The shape of the calorimetrically observed curve resembles the one from Raman data for a cut-off frequency of  $6 \text{ cm}^{-1}$ . The Raman values are actually smaller by about 20%. An attempt to fit our Raman data to the calorimetric values gives a fitting value of  $N = 3.12 \times 10^{21} \text{ g}^{-1}$  assuming that the Debye contribution is  $(C/T^3)_D = 1.73 \times 10^{-5} \text{ J(g K}^4)^{-1}$ . The very low temperature part of the curve that cannot be predicted from Raman measurements seems likely to originate from modes of much lower frequency than the ones observed in the Raman scattering spectrum.

The depolarized low frequency Raman reduced spectrum of PMMA is resolved into two bands, a broad strong band at about  $91 \text{ cm}^{-1}$  and a weak narrow band at about  $22 \text{ cm}^{-1}$ . The high frequency band has been previously observed in neutron scattering<sup>33</sup>, by far infrared absorption by Tadokoro *et al.*<sup>38</sup>, and it has also been predicted by fitting thermal conductivity data above 90 K to Tarasov's model process<sup>39</sup>. The low frequency weak band has been observed in dielectric relaxation measurements<sup>40</sup> infra-red measurements<sup>41</sup> and theoretically predicted<sup>39</sup>.

Various interpretations assign the high frequency band to the side group motion of the chain and Debye frequencies calculated for this band support the side group libration assumption. Such evidence leads us to assume that it is phonon-like waves transferring heat in the amorphous solid polymers. Additional unpublished Raman data from other amorphous polymers agree with

the above assumption. The low frequency narrow band at about  $22 \text{ cm}^{-1}$  could not be predicted by Debye theory. This latter peak is typical in most of the other amorphous solid polymers we have so far studied. The frequency decreases with increasing side group fractional mass in the repeat unit and appears more intense in polymers with rigid backbone chains. Relating this peak at very low frequencies with the backbone contribution to the motion of the chain as a whole seems therefore a reasonable explanation.

We can adopt therefore the models concerning the Debye-like phonons in glasses existing as heat carriers to explain the very low temperature specific heat anomaly combined with the low frequency Raman spectral data. In crystals the heat is transferred by lattice vibrations. In amorphous solids the dispersion relations are complicated because of a larger number of phonon-like frequencies  $\omega$  for every wave vector. The increased number of heat carrier modes lead to a higher than expected specific heat at low temperatures and are seen in the low frequency Raman spectrum as a broad band. It has been suggested that the Debye-like phonons are scattered by excitations that could well be represented by two-level systems<sup>42,43</sup>. Below 1 K possible tunnelling phenomena<sup>44,45</sup> will increase the number of modes and

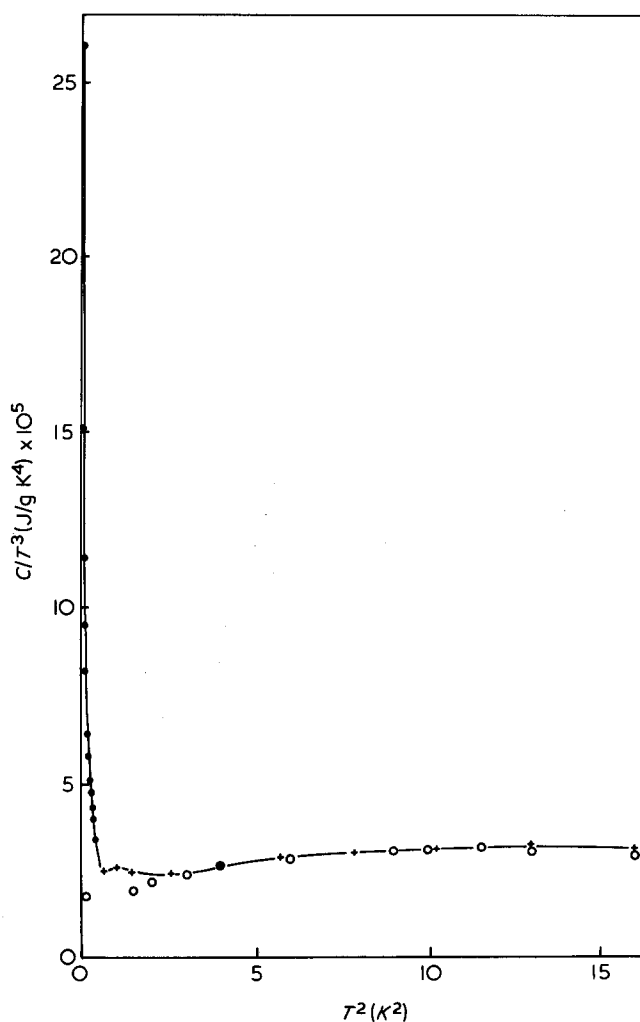


Figure 12 Specific heat of amorphous PMMA. (○) Raman data, present work, (●) data from Stephens<sup>21</sup>, (+) data from Choy *et al.*<sup>18</sup>

therefore the specific heat rises to even higher values. In the amorphous solid with no structural order the low frequency region may be treated in a quasi-elastic approximation. The individual polymer side group dynamics may be coupled to the main chain motions and appear in the low frequency Raman spectrum.

Electron microscopy has revealed the existence of local order in the amorphous phase which is believed to result from the conditions of preparation<sup>46</sup>. Dean considered a picture of localized lattice modes in disordered systems where the extent of localization depends on the degree of disorder<sup>47</sup>. Phonon-like heat carrying waves reflect the low frequency motions inside the chain, mainly the backbone motion and the side group motion in polymers possessing a side group in their repeat unit. We believe that it is likely that the low frequency Raman spectrum contains only the high frequency part of the density of states (obviously the larger part) of these phonon-like vibrations. The calculated specific heat yields therefore values smaller than those measured calorimetrically at low temperatures  $\approx 1$  K.

#### ACKNOWLEDGEMENTS

Our thanks are extended to Dr Frank Heatley for taking the n.m.r. spectra, Dr T. G. Swales for help with X-ray diffraction measurements on certain samples and Mr. Derek Roy for g.p.c. data. We wish to thank Dr J. Yarwood and Dr G. O'Neil of the Science Laboratories of Durham University for measurements of far infra-red absorption spectra.

#### REFERENCES

- 1 Flubacher, P., Leadbetter, A. J., Morrison, J. A. and Stoicheff, B. *P. J. Phys. Chem. Solids* 1959, **12**, 53
- 2 Krishnan, R. S. *Proc. Ind. Acad. Sci.* 1953, **A37**, 377
- 3 Stolen, R. H. *Phys. Chem. Glasses* 1970, **3**, 83
- 4 Furukawa, T., Fox, K. E. and White, W. B. *J. Chem. Phys.* 1981, **75**, 3226
- 5 Hass, M. J. *Phys. Chem. Solids* 1970, **31**, 415
- 6 Roy, N. K. *Ind. J. Phys.* 1953, **27**, 167
- 7 Kim, J. J., McLeish, J., Hyde, A. J. and Bailey, R. T. *Chem. Phys. Lett.* 1973, **22**, 503
- 8 Spells, S. J. and Shepherd, I. W. *J. Chem. Phys.* 1977, **66**, 1427
- 9 Spells, S. J. and Shepherd, I. W. in 'Structure of Non-Crystalline Materials' (Ed. P. H. Gaskell) 1977, p 145
- 10 Sankaranarayanan, V. N., Bailey, R. T. and Hyde, A. J. *Spec. Acta* 1978, **34A**, 387
- 11 Perrot, M., Brooker, M. H. and Lascombe, J. J. *Chem. Phys.* 1981, **74**, 2787
- 12 Nielson, O. F. and Lund, P. A. *Chem. Phys. Lett.* 1981, **78**, 626
- 13 Nielsen, O. F. *Chem. Phys. Lett.* 1979, **66**, 350
- 14 Debye, P. *Ann. Physik*, 1912, **39**, 789
- 15 Leadbetter, A. J. *Phys. Chem. Glasses* 1968, **9**, 1
- 16 Anderson, O. L. *J. Phys. Chem. Solids* 1959, **12**, 41
- 17 Antoniou, A. A. and Morrison, J. A. *J. Appl. Phys.* 1965, **36**, 1873
- 18 Choy, C. L., Hunt, R. G. and Salinger, G. L. *J. Chem. Phys.* 1970, **52**, 3629
- 19 Salinger, G. L. in 'Amorphous Materials' (Eds R. W. Douglas and B. Ellis) Wiley 1970, p 475
- 20 Zeller, R. C. and Pohl, R. O. *Phys. Rev.* 1971, **B4**, 2029
- 21 Stephens, R. B. *Phys. Rev.* 1973, **B8**, 2896
- 22 Stephens, R. B. *Phys. Rev.* 1976, **B13**, 852
- 23 Pohl, R. O. in 'Topics of Current Physics'. Amorphous Solids—Low Temperature Properties' (Ed. W. A. Phillips) 1981, **24**, 27
- 24 Shuker, R. and Gammon, R. W. *Phys. Rev. Lett.* 1970, **25**, 222
- 25 Lannin, J. S. *Solid State Comm.* 1972, **11**, 1523
- 26 Lannin, J. S. *Solid State Comm.* 1973, **12**, 947
- 27 Whalley, E. and Bertie, J. E. *J. Chem. Phys.* 1967, **46**, 1264
- 28 Cowly, R. A. *Rep. Prog. Phys.* 1968, **31**, 123
- 29 Fraser, G. V. *Polymer* 1978, **19**, 857
- 30 Snyder, R. G., Krause, S. J. and Scherer, J. R. *J. Polym. Sci. Polym. Phys. Edn.* 1978, **16**, 1593
- 31 Spells, S. J., Shepherd, I. W. and Wright, C. J. *Polymer* 1977, **18**, 905
- 32 Brier, P. N., Higgins, J. S. and Bradley, R. H. *J. Mol. Phys.* 1971, **21**, 721
- 33 Higgins, J. S., Allen, G. and Brier, P. N. *Polymer* 1972, **13**, 157
- 34 Anderson, O. L. *J. Phys. Chem. Solids* 1959, **12**, 41
- 35 Wunderlich, B. and Baur, H. *Adv. Polym. Sci.* 1970, **7**, 151
- 36 To be published
- 37 Spells, S. J. and Shepherd, I. W. *Chem. Phys. Lett.* 1977, **45**, 606
- 38 Tadokoro, H., Chatani, Y., Kusanagi, H. and Yokohana, M. *Macromolecules* 1970, **3**, 441
- 39 Reese, W. J. *Appl. Phys.* 1966, **37**, 3227
- 40 Miller, S., Tomozawa, T. and McCrone, R. K. in 'Amorphous Materials' (Eds R. W. Douglas and B. Ellis) Wiley, 1970, p 89
- 41 Manley, T. R. and Martin, C. G. *Polymer* 1971, **12**, 524
- 42 Hunklinger, S., Arnold, W., Stein, S., Nava, R. and Dransfield, K. *Phys. Lett.* 1972, **A42**, 253
- 43 Golding, B., Graebner, J. E., Halperin, B. I. and Schultz, R. J. *Phys. Rev. Lett.* 1976, **30**, 223
- 44 Anderson, P. W., Halperin, B. I. and Varma, G. *Phil. Mag.* 1972, **25**, 1
- 45 Phillips, W. A. *J. Low Temp. Phys.* 1972, **7**, 351
- 46 Stevens, G. S., Champion, J. V. and Liddell, P. J. *Polym. Sci. Polym. Phys. Edn.* 1982, **20**, 327
- 47 Dean, P. *Proc. Phys. Soc.* 1964, **84**, 727